BBA - Biomembranes 1864 (2022) 183977

Contents lists available at ScienceDirect

BBA - Biomembranes

journal homepage: www.elsevier.com/locate/bbamem

Ivermectin and curcumin cause plasma membrane rigidity in *Leishmania amazonensis* due to oxidative stress

Lais Alonso [a], Miriam Leandro Dorta [b], Antonio Alonso [a,*]

[a] Instituto de Física, Universidade Federal de Goiás, Goiânia, GO, Brazil
[b] Instituto de Patologia Tropical e Saúde Publica, Departamento de Imunologia e Patologia Geral, Universidade Federal de Goiás, Goiânia, GO, Brazil

ARTICLE INFO

Keywords:
Ivermectin
Curcumin
Leishmania
Drug repositioning
electron paramagnetic resonance

ABSTRACT

Spin label electron paramagnetic resonance (EPR) spectroscopy was used to study the mechanisms of action of ivermectin and curcumin against *Leishmania (L.) amazonensis* promastigotes. EPR spectra showed that treatment of the parasites with both compounds results in plasma membrane rigidity due to oxidative processes. With the IC_{50} and EPR measurements for assays using different parasite concentrations, estimations could be made for the membrane-water partition coefficient ($K_{M/W}$), and the concentration of the compound in the membrane (c_{m50}) and in the aqueous phase (c_{w50}), which inhibits cell growth by 50%. The $K_{M/W}$ values indicated that ivermectin has a greater affinity than curcumin for the parasite membrane. Therefore, the activity of ivermectin was higher for experiments with low cell concentrations, but for concentrations greater than 1.5×10^8 parasites/mL the compounds did not show significantly different results. The c_{m50} values indicated that the concentration of compound in the membrane leading to growth inhibition or membrane alteration is approximately 1 M for both ivermectin and curcumin. This high membrane concentration suggests that many ivermectin molecules per chlorine channel are needed to cause an increase in chlorine ion influx.

1. Introduction

The leishmaniases are a group of tropical neglected diseases caused by more than 20 species of the protozoan parasite *Leishmania*. According to the World Health Organization (WHO) [1], the leishmaniases are endemic in 98 countries around the world, with more than 1 billion people living in these endemic areas and that are at risk of infection. Each year there are around 30,000 new cases of visceral leishmaniasis and over 1 million new cases of cutaneous leishmaniasis [1]. In Brazil, *Leishmania (Viannia) braziliensis* and *Leishmania (Leishmania) amazonensis* are considered the most epidemiologically relevant species, both of which manifest as cutaneous leishmaniasis [2]. The typical treatments for leishmaniasis involve pentavalent antimonials, amphotericin B, miltefosine, and paromomycin [2]; however these have high toxicity and require long treatment duration, in addition there has been an emergence of drug resistance [3]. Drug repositioning is a favorable option in the search for new antileishmanial treatments due to the fact that the discovery of new drugs is a long and expensive process [4].

Ivermectin is a broad-spectrum drug used for the treatment of parasitic diseases including head lice, scabies, river blindness (onchocerciasis), and ascaris lumbricoides [5,6]. Oral use of ivermectin in humans is FDA-approved for the treatment of intestinal strongyloidiasis and onchocerciasis, while its topical use is FDA-approved to treat external parasites like lice and for skin conditions like rosacea [7]. In Brazil, ivermectin is approved for anti-parasitic use in humans under medical prescription (ANVISA Registration No. 1039201670020, Authorization 1003923, Process 25351.217020/2010-23, Validity 11/01/2025). In addition, ivermectin is a drug widely used in veterinary medicine [7]. Under experimental conditions, ivermectin has been reported to have antiparasitic activity against leishmaniasis [4], trypanosomiasis [8,9], and malaria [10]. Ivermectin activates glutamate-gated chloride channels in the parasite, resulting in chloride ion influx and plasma membrane hyperpolarization [11–13]. In recent years, an increasing number of studies have indicated that ivermectin may have wide use in the treatment of different types of cancer, but the mechanisms of this anti-cancer activity remain unclear [13–15]. Interestingly, several studies have shown that ivermectin increases intracellular reactive oxygen species (ROS) production and alters mitochondrial membrane potential [4,6,13–15]. For example, it has been shown that ivermectin selectively kills chronic myeloid leukemia cells by causing mitochondrial dysfunction and inducing oxidative stress [14]. Normal cells appear to have a greater ability to cope with ROS-generating

* Corresponding author.
E-mail address: alonso@ufg.br (A. Alonso).

https://doi.org/10.1016/j.bbamem.2022.183977
Received 18 March 2022; Received in revised form 18 May 2022; Accepted 26 May 2022
Available online 30 May 2022

compounds than cancer cells, and thus, cancer cells are likely preferentially targeted and killed by these compounds [16,17].

Curcumin is a diferuloylmethane, which is the major yellow bioactive component of turmeric (*Curcuma longa*), a member of the ginger family, *Zingiberaceae*. Curcumin has demonstrated a broad spectrum of biological action, including in vitro leishmanicidal activity [18–20]. The molecule is well tolerated in humans, but its low oral bioavailability is a disadvantage that limits its use as a potential chemotherapeutic agent [21]. It is documented that curcumin is a scavenger of ROS, such as the hydroxyl radical and superoxide anion, and has been shown to inhibit lipid peroxidation [22]. On the other hand, curcumin induces hyperproduction of ROS in several species of *Leishmania* [19–21]. The resulting oxidative stress is associated with mitochondrial membrane depolarization, which may cause lipid peroxidation and apoptosis-like death [19].

Electron paramagnetic resonance (EPR) spectroscopy associated with the spin label method has been shown to be the technique of choice to study molecular dynamics in biological membranes. This technique has already been used to investigate the interactions of antileishmanial compounds, for which the mechanisms of action were not elucidated, with the plasma membrane of the parasite. Miltefosine has been shown to cause remarkable increases in membrane fluidity, acting mainly on the membrane protein component [23–25], while terpenes, such as nerolidol, also increase fluidity, they appear to act on the lipid component [26,27]. After treatment with amphotericin B, membrane rigidity occurs due to the interactions of the spin labels with the hydrophobic surface of the putative aggregates formed by the drug [28,29]. Lipoperoxidation and protein oxidation also cause membrane rigidity, but their effects are easily discernible from those caused by the physical presence of drugs in the membrane. Whereas the effects caused by the drug are observed soon after addition, the effects caused by oxidative stress increase significantly with the incubation period.

Recently, it has been reported that several ROS-forming leishmanicidal compounds cause cell membrane rigidity. It has been shown that the treatment of *L. amazonensis* promastigotes with chalcone [30], β-carboline-oxazoline [31,32], and other isoxazoles [33] derivatives cause rigidity of the plasma membrane due to oxidative stress. Furthermore, in *Trypanosoma cruzi*, a parasite of the same family as *Leishmania*, treatment with sesquiterpene (−)-elatol caused membrane rigidity [34]. Interestingly, for all these compounds, antiparasitic activity was associated with ROS formation, increased superoxide anion production, and mitochondrial membrane depolarization.

Given the fact that ivermectin causes an increase in the influx of chlorine ion, thereby increasing the formation of intracellular ROS and causing the depolarization of the mitochondrial membrane, this suggests that other leishmanicidal compounds that also produce these intracellular effects in the parasite could have a primary action on the plasma membrane by altering its electrolyte permeation. Since other ROS-forming compounds, such as the chalcone [30] and β-carboline-oxazoline derivatives [31,32], have already been shown to cause membrane rigidity in *Leishmania* parasites, in the current study we investigate whether ivermectin, as well as curcumin, likewise cause membrane rigidity in the *L. amazonensis* parasite. In addition, we used a methodology described in previous works [24,25,27,29–32] to assess the membrane-water partition coefficient of the compounds, as well as their membrane concentrations that inhibit 50% of the parasite growth. These biophysical parameters allowed us to analyze the affinities that ivermectin and curcumin have for the parasite membrane and in what amounts they accumulate in the membrane to exert their activities.

2. Materials and methods

2.1. Chemicals

Ivermectin (CAS number: 70,288-86-7, MW: 875.09 g/mol, purity >90%), curcumin from *Curcuma longa* (Turmeric) (CAS number: 458-37-7, MW: 368.38 g/mol, purity >65%), Grace's insect medium, L-glutamine, penicillin G, streptomycin, hygromycin B, 3-(4,5-dimethylthiazol-2-yl)-2,5-diphenyl tetrazolium bromide (MTT), and 5-doxyl stearic acid (5-DSA) were purchased from Sigma-Aldrich (St. Louis, MO, USA). Heat-inactivated fetal bovine serum (FCS) was purchased from Corning Life Sciences (NY, USA).

2.2. Parasite cells

Leishmania (Leishmania) amazonensis (MHOM/BR/75/Josefa) reference strain was cultured in the promastigote form in 24-well culture plates containing 2 mL Grace's insect medium supplemented with 20% FCS, 100 U/mL penicillin G, 100 μg/mL streptomycin, and 2 mM L-glutamine, at 26 °C, in anaerobic conditions as previously described [27–30]. Parasites in the stationary phase of growth (6th day of culture), according to previously published data [23–26], were used in the assays.

2.3. In vitro assays of antiproliferative activity

In 96-well culture plates, *L. amazonensis* promastigotes (at either 1×10^7, 1×10^8, or 5×10^8 parasites/mL in Grace's medium supplemented with 10% FCS) were treated with increasing concentrations of ivermectin or curcumin in a total volume of 100 μL per well. After an incubation period of 24 h at 26 °C, cell viability was assessed based on the conversion of water-soluble MTT to formazan by viable mitochondria, after a period of 2–5 h in the dark, as described by other works [23–30]. The percentage of viable cells for each compound concentration was determined by the absorbance of formazan at 540 nm and the half-maximal inhibitory concentration (IC_{50}) values of ivermectin and curcumin were then determined by fitting a sigmoid curve to the concentration-response data [29,30].

2.4. EPR spectroscopy

EPR experiments were performed similar to the antiproliferative assays, but with samples containing a higher number of parasites (~1×10^8/sample). *L. amazonensis* promastigotes were diluted in Grace's medium in 24-well culture plates (final cell concentrations of 2×10^7, 5×10^7, 1.5×10^8, 5×10^8, and 1.25×10^9 parasites/mL). The concentrations of ivermectin or curcumin used ranged between 10 and 500 μM. After 24 h of incubation at 26 °C the cells were centrifuged at 1800 ×*g* for 10 min, the supernatant was discarded and the cells were resuspended in 50 μL of phosphate-buffered saline (PBS). For the spin labeling of the plasma membrane, first a film of the spin label 5-DSA was prepared at the bottom of a glass tube using a 1 μL aliquot of the 5-DSA dissolved in ethanol (4 mg/mL). After evaporation of the solvent, the cells (1×10^8 parasites suspended in 50 μL PBS) were added to the spin label film and the test tube was gently stirred. The cell suspension was introduced into a 1-mm-i.d. capillary tube, which was flame sealed. Before measuring the EPR, the capillary was centrifuged at 15000 ×*g* for 5 min to improve the signal-to-noise ratio.

The EMX-Plus spectrometer from Bruker (Rheinstetten, Germany) was used to record the EPR spectra, operating in the following instrumental configurations: microwave power, 10 mW; microwave frequency, 9.452 GHz; modulation frequency, 100 kHz; modulation amplitude, 1.0G; magnetic field sweep, 100G; scan time, 168 s; and sample temperature, 25 °C.

2.5. Data processing

Each experiment was conducted at least three independent times and the data are expressed as mean and standard deviation. A one-way analysis of variance (ANOVA) with Tukey's test was used to identify significant differences ($P < 0.05$) between means among the different treatments.

3. Results

3.1. Ivermectin and curcumin cause plasma membrane rigidity in the parasite

Fig. 1 shows the EPR spectra of the lipid spin label 5-DSA inserted in the plasma membrane of *L. amazonensis* promastigotes for untreated samples and samples treated with different concentrations of ivermectin and curcumin. With the increase in the concentration of the compounds, a gradual increase in the EPR $2A_{//}$ parameter is observed, indicating remarkable reductions in membrane fluidity. For 24-h assays using a parasite concentration of 5×10^7 per mL, the presence of 10 μM ivermectin or 20 μM curcumin in the culture medium was sufficient to produce an increase in $2A_{//}$ above the experimental error of 0.5 G (Fig. 1a and b). Using an incubation period of only 4 h, the effects of the compounds were reduced, requiring higher concentrations of the compounds for the membrane rigidity effects to be observed (Fig. 1c). By increasing the concentration of cells used in the assay by 5 times (1.25×10^9 parasites/mL) the concentrations of compounds needed to observe membrane changes were also much higher (Fig. 1d).

3.2. EPR results correlate with antiproliferative effects

The IC_{50} values of ivermectin and curcumin for *L. amazonensis* promastigotes were dependent on the cell concentration used in the MTT assay (Table 1). Table 1 also presents the minimum concentrations of ivermectin and curcumin required for an observable change in the EPR spectra of 5-DSA. For different cell concentrations, the EPR measurements were performed at different concentrations of compounds to find the lowest compound concentration that caused an increase in $2A_{//}$ greater than 0.5 G, its experimental error. With the increase in cell concentration used in the assay, there was a significant increase in the compound concentrations that led to the antiproliferative and membrane effects.

In this work, we used curcumin obtained from Sigma, which has a purity content of 65% (concentrations were calculated based on this

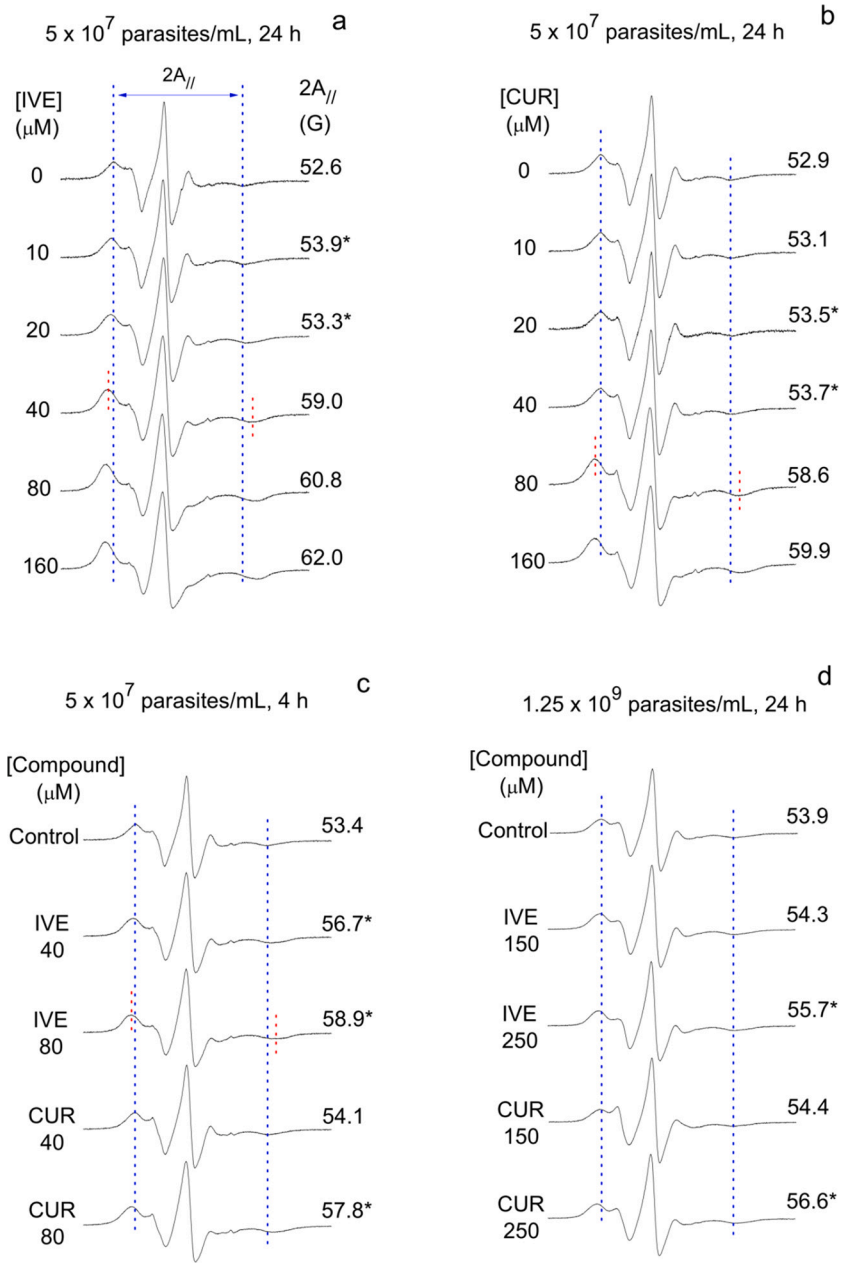

Fig. 1. EPR spectra of spin label 5-DSA in the plasma membrane of *Leishmania amazonensis* promastigotes for samples of different concentrations of ivermectin (IVE) and curcumin (CUR). To the right of each spectrum are the values of the EPR parameter $2A_{//}$ (outer hyperfine splitting), which is the magnetic field separation between the first peak and the last inverted peak of the spectrum. The * represents values of $2A_{//}$ with a difference greater than 0.5 G (estimated experimental error) in relation to the control value. Panel (c) shows EPR spectra for treatments of 4 h and panel (d) shows EPR spectra for experiments with the highest concentration of cells used. In all EPR spectra the total scan range of the magnetic field was 100 G (X axis), and the intensity is in arbitrary units (Y axis).

Table 1
IC_{50} values and minimum concentration for an EPR-detectable membrane change for ivermectin and curcumin at different concentrations of *L. amazonensis* promastigotes used in the assay.

[Cell] (1×10^8 cells/mL)	Ivermectin	Curcumin
IC_{50} (μM)		
0.1	8.1 ± 3.2 (A)[a]	20.2 ± 8.4 (A)
1	19.3 ± 3.9 (B)	31.5 ± 11.5 (A)
5	73.4 ± 22.2 (C)	81.9 ± 30.2 (B)
EPR (μM)		
0.2	9.9 ± 2.2 (A)	18.2 ± 7.4 (A)
0.5	13.4 ± 3.6 (A)	22.8 ± 8.9 (A)
1.5	28.1 ± 3.5 (B)	35.1 ± 11.8 (A)
5	82.7 ± 15.8 (C)	70.7 ± 26.5 (B)
12.5	240.8 ± 50.5 (D)	208.6 ± 83.7 (C)

[a] Statistical significance: for each data set in each column, means indicated with same capital letter are not significantly different at $P < 0.05$.

curcumin content). Das et al. (2008) [19] evaluated the activity of curcumin obtained from Sigma against promastigotes of *L. donovani* and found a 50% reduction in cell viability at a curcumin concentration of approximately 25 μM. This result is similar to the IC_{50} value of 20.2 ± 8.4 μM (Table 1) for *L. amazonensis* promastigotes at a cell concentration of 1×10^7 cells/mL.

These data for different concentrations of the parasite allowed us to obtain three important biophysical parameters associated with the plasma membrane, which are: the membrane-water partition coefficient, $K_{M/W}$, and the concentrations of the compounds in the aqueous phase, c_{w50}, and in the membrane, c_{m50}.

The dependence of IC_{50} values on assay cell concentration occurs because hydrophobic molecules accumulate in the cell membrane in high concentrations, making their distribution in the suspension inhomogeneous. For samples that are diluted or have low cell concentrations, the amount of membrane in the suspension is negligible and the drug concentration in the suspension is practically equal to that of the aqueous medium. But when the cell concentration of the sample is high, a substantial fraction of the compound goes to the membrane so that its concentration in the aqueous phase is much lower than in the suspension. The equation that describes the variation of IC_{50} with cell concentration has previously been reported [28,29], and it is as follows:

$$IC_{50} = \left[\frac{(V_{mc} \cdot c_c)^{-1} + K_{M/W}}{(V_{mc} \cdot c_c)^{-1} + 1}\right] c_{w50} \quad (1)$$

V_{mc} is the estimated cell membrane volume for the L. *amazonensis* promastigote (8.17×10^{-13} mL) [24] and c_c is the number of cells per mL. As the biophysical parameters $K_{M/W}$ and c_{w50} are covariant in Eq. (1), they can be determined by fitting the curve provided by this equation to experimental data of IC_{50} versus c_c. Furthermore, as $K_{M/W} = c_{w50}/c_{m50}$, the c_{m50} value can be determined. In order to obtain the biophysical parameters the IC_{50} and EPR data shown in Table 1 were plotted for the different cell concentrations (Fig. 2). The best-fit curves shown in Fig. 2 were obtained using Eq. (1) and from these curves the best-fit parameters were determined. The curves on the EPR data were also obtained using Eq. (1), where the dependent variable IC_{50} can be replaced by C_{EPR}, representing the compound concentration for an EPR-detectable change, and the best-fit parameters c_{w50} and c_{m50} can be denoted by c_{wEPR} and c_{mEPR}, respectively.

The biophysical parameters obtained are shown in Table 2. Interestingly, the parameters obtained from the IC_{50} values were essentially the same as those obtained from the EPR data. These results suggest that the antiproliferative effects of the studied compounds are associated with the plasma membrane rigidity of the parasite. From the $K_{M/W}$ values it can be inferred that the membrane affinity of ivermectin is much higher than that of curcumin. However, the membrane compound concentration leading to 50% inhibition of parasite growth (c_{w50}) did not differ significantly for ivermectin and curcumin. This parameter also indicated that a very high membrane compound concentration of approximately 1 M is required for growth inhibition or membrane alteration.

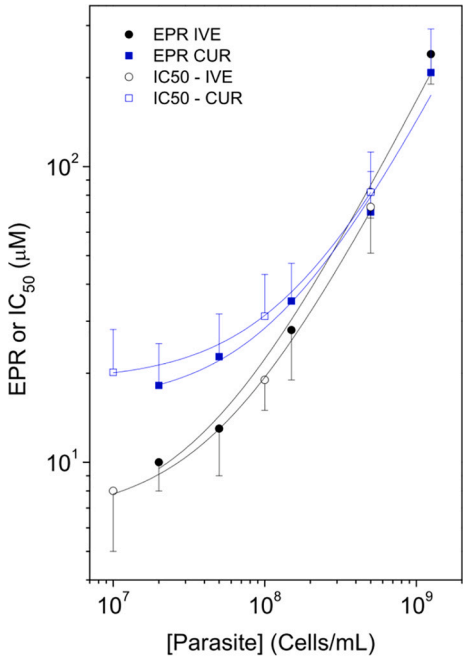

Fig. 2. IC_{50} values and minimum compound concentration for an observable plasma membrane change detected by EPR for ivermectin (IVE) and curcumin (CUR) in the different assay concentrations of *L. amazonensis* promastigotes (C_{EPR}). The EPR curves indicate concentrations of ivermectin and curcumin necessary to cause a change in the $2A_{//}$ parameter of 5-DSA (~0.5 G). The best-fit curves shown are based on Eq. (1).

Table 2
Biophysical parameters $\mathbf{K_{M/W}}$, c_{w50}, and c_{m50} calculated from interactions of **ivermectin** and curcumin with the plasma membranes of *L. amazonensis* promastigotes.

Compound	$K_{M/W}$ (10^4)[a]	Log $K_{M/W}$	c_{w50} (μM)	c_{m50} (M)
Ivermectin	15.1 ± 1.5 (A)[b]	5.18	6.5 ± 0.5 (A)	0.98 ± 0.12 (A)
Curcumin	5.5 ± 0.8 (B)	4.74	18.8 ± 0.9 (B)	1.03 ± 0.15 (A)
Chalcone[c]	10.2 ± 0.9	5.01	6.8 ± 1.6	0.69 ± 0.19
	EPR			
			c_{wEPR} (μM)	**c_{mEPR} (M)**
Ivermectin	19.6 ± 4.0 (A)	5.29	6.3 ± 1.0 (A)	1.23 ± 0.32 (A)
Curcumin	6.2 ± 1.2 (B)	4.79	15.7 ± 1.8 (B)	0.98 ± 0.22 (A)

[a] Best-fit parameters obtained by fitting of Eq. (1) to the experimental data from Fig. 2.
[b] Statistical significance: in each column, data indicated with same capital letter are not significantly different at $P < 0.05$.
[c] Data from previous work with a chalcone derivative [30] are shown for comparison.

For diluted samples, the c_{w50} values of the compounds indicated that ivermectin is much more efficient than curcumin in inhibiting parasite growth. However, for assays with higher cell concentrations ($>1.5 \times 10^8$ parasites/mL) the IC_{50} or C_{EPR} values do not differ significantly (Fig. 2 and Table 1). This result shows that for low cell concentrations the higher membrane affinity of ivermectin provides an advantage, but this advantage disappears for assays with higher cell concentrations. It is important to consider that experiments with higher cell concentrations are more physiologically relevant since throughout the human body the cellular concentrations are high.

4. Discussion

It is well known that with an augmented production of the mitochondrial superoxide anion, other ROS and lipid oxidation products are formed during the peroxidation of ω-6 polyunsaturated fatty acids (PUFAs) (linoleic, γ-linolenic, and arachidonic acid) [35–37]. Throughout the subsequent chain of free radical reactions, the formation of several reactive aldehydes occurs and, among these lipid peroxidation products, 4-hydroxy-2-nonenal (4-HNE) represents one of the most bioactive and well-studied lipid alkenals [37,38]. 4-HNE covalently modifies phosphatidylethanolamine (PE) to form different 4-HNE-PE adducts, being responsible for increasing the permeability of sodium ions in the membrane [37]. As an amphiphilic compound, 4-HNE tends to concentrate on biomembranes where it can react not only with PE, but also with membrane proteins, such as transporters, ion channels, and receptors [39]. Protein conformational changes mediated by 4-HNE are usually attributed to their capacity to modify molecules by binding covalently to Cys, Lys, and His residues of protein [37,39–41]. Although it has been shown that 4-HNE does little to change the fluidity of lipid bilayer of liposomes made from *Escherichia coli* lipid [40], it was recently reported [42] that treatment of *L. amazonensis* promastigotes with 4-HNE causes membrane rigidity in the parasite to such an intense degree as shown here for ivermectin and curcumin, likewise for the chalcone [30] and β-carboline-oxazoline [31,32] derivatives of other studies. Furthermore, the EPR spectra of the parasite treated with 4-HNE were very similar to those presented here for the two studied compounds.

The degree of membrane rigidity caused by the treatment of the parasite with ivermectin or curcumin was very high, suggesting the involvement of cross-linking formation between membrane proteins. Similar EPR spectra of spin label 5-DSA inserted into plasma membrane were observed for erythrocytes oxidized with hydrogen peroxide in a phosphate buffer with azide, a catalase inhibitor [43]. Through treatment of erythrocytes with 200 μM H_2O_2, the parameter $2A_{//}$ reached values close to 60 G, showing a large increase of ~4 G [43]. Furthermore, it has been shown by Snyder and coauthors (1985) that, under this treatment condition, hydrogen peroxide induces the formation of cross-linking between hemoglobin and human erythrocyte skeletal proteins [44]. Spin label EPR spectroscopy has been demonstrated as an important method to detect the occurrence of lipid and protein peroxidation in biological membranes [45,46]. Cross-linking between lipids, as well as intra- and inter-membrane protein binding, leads to membrane rigidity [44]. In model membranes the changes due to lipid peroxidation are generally minor [40], but in cell membranes, increases in the $2A_{//}$ parameter of up to ~2 G have been observed after lipid peroxidation [45,46], and increases of up to ~5 G have been observed when cross-linking occurs between membrane proteins [44].

The octanol-water partition coefficient (Log $P_{O/W}$) for ivermectin and curcumin have been reported to be 3.57 [47] and 3.22 [48], respectively. The fact that the Log $K_{M/W}$ values for ivermectin and curcumin found here are much higher (5.18 and 4.74, Table 2) indicates that these compounds have much greater affinities for the *Leishmania* membrane than for octanol, and one of the reasons may be related to the interactions of these compounds with membrane proteins.

Membrane-water partition coefficient measurements indicated that ivermectin has more affinity for the *L. amazonensis* membrane than curcumin, as deduced from the $K_{M/W}$ values (Table 2). For this reason, ivermectin showed greater activity than curcumin for assays with low cell concentrations (Fig. 2). However, this advantage disappeared for higher cell concentrations. From 1.5×10^8 parasites/mL, the two compounds did not show significant differences. For diluted samples the aqueous phase of the suspension has a large volume and a larger fraction of the compound with lower membrane affinity remains in the aqueous medium. Assays with higher cell concentrations are physiologically more relevant. For example, in blood the cell concentration is approximately 5×10^9 cells/mL and thus there is a large volume of membrane where hydrophobic molecules can be incorporated. In an infected tissue, the cell concentration is also high, and it is important to consider that, regardless of the number of *Leishmania* parasites in relation to the cells of the tissue, the partitioning into the membrane will be similar to what was found in this work, assuming that the interstitial aqueous medium has properties similar to those of culture medium used in the assays. Thus, our results suggest that when the concentration of the compound in the interstitial fluid is equal to c_{w50} (Table 2), the expected concentration in the parasite membrane would be similar to the corresponding value of c_{m50}. However, in the case of the amastigote form of the parasite inside the macrophage, the $K_{M/W}$ partition coefficient of each compound would depend on its affinity for the plasma membrane of the amastigote and on its interactions with the aqueous medium within the parasitophorous vacuole.

From the c_{m50} values the concentration of ivermectin or curcumin in the plasma membrane that inhibits parasite growth by 50% was deduced to be approximately 1 M (Table 2). Such a high concentration of ivermectin in the membrane suggests that there are a large number of molecules available in the membrane to interact with chlorine channels. It is possible that many ivermectin molecules per chlorine channel are required to cause the increase in chlorine ion influx sufficient to compromise parasite growth. In addition, the fact that our results were found to be similar for ivermectin and curcumin, except for assays with low cell concentrations, suggests that the mechanisms of these compounds could also be similar. More studies would be needed to verify if curcumin interacts with an ion channel in the plasma membrane of the parasite and thus increase its passive ionic transport. An alteration in the cell's resting potential could cause a change in the mitochondrial membrane potential and thus lead to increased ROS production that has been observed for both of these compounds.

5. Conclusions

EPR spectroscopy showed that treatment of *L. amazonensis* promastigotes with ivermectin or curcumin causes plasma membrane rigidity due to oxidative stress. Ivermectin showed greater affinity for the parasite membrane than curcumin, which resulted in lower IC_{50} values for assays with low cell concentration. However, for higher cell concentrations the compounds did not show significant differences. The concentrations of these compounds in the plasma membrane that led to a reduction in parasite growth or a change in the EPR spectrum were quite high (~1 M). For ivermectin this result suggests that many molecules per chlorine channel are required to generate an increase in ionic flux. For curcumin, further studies are needed to determine if it can sufficiently affect any of the ion channels of the parasite. This work also shows the therapeutic possibility of targeting uncontrolled ionic transport in the plasma membrane of *Leishmania* parasites.

Declaration of competing interest

The authors declare that they have no known competing financial interests or personal relationships that could have appeared to influence the work reported in this paper.

Acknowledgements

This study was financially supported by grants from the Brazilian research funding agencies CNPq (445666/2014-5 and 406521/2016-6), CAPES and FAPEG (201210267001110). Lais Alonso was a recipient of a postdoctoral fellowship from CNPq (150369/2018-2) and is currently a postdoctoral fellow at CAPES. Antonio Alonso received a research grant from CNPq (304122/2019-0).

References

[1] World Health Organization, Leishmaniasis. http://www.who.int/topics/leishmaniasis/en/, 2018. (Accessed 29 December 2021).

[2] S.M. Christensen, A.T. Belew, N.M. El-Sayed, W.L. Tafuri, F.T. Silveira, D. M. Mosser, Host and parasite responses in human diffuse cutaneous leishmaniasis caused by L. amazonensis, PLoS Negl Trop Dis 13 (3) (2019), e0007152, https://doi.org/10.1371/journal.pntd.0007152.

[3] J. Chakravarty, S. Sundar, Current and emerging medications for the treatment of leishmaniasis, Expert. Opin. Pharmacother. 20 (10) (2019) 1251–1265, https://doi.org/10.1080/14656566.2019.1609940.

[4] T.A.R. Reis, J.A. Oliveira-da-Silva, G.S.V. Tavares, D.V.C. Mendonça, C.S. Freitas, R.R. Costa, D.P. Lage, V.T. Martins, A.S. Machado, F.F. Ramos, A.M. Silva, F. Ludolf, L.M.R. Antinarelli, R.C.F. Brito, M.A. Chávez-Fumagalli, M.V. Humbert, B.M. Roatt, E.S. Coimbra, E.A.F. Coelho, Ivermectin presents effective and selective antileishmanial activity in vitro and in vivo against leishmania infantum and is therapeutic against visceral leishmaniasis, Exp. Parasitol. 221 (2021), 108059, https://doi.org/10.1016/j.exppara.2020.108059.

[5] E.A. Ottesen, W.C. Campbell, Ivermectin in human medicine, J. Antimicrob. Chemother. 34 (2) (1994) 195–203, https://doi.org/10.1093/jac/34.2.195.

[6] M. Juarez, A. Schcolnik-Cabrera, A. Dueñas-Gonzalez, The multitargeted drug ivermectin: from an antiparasitic agent to a repositioned cancer drug, Am. J. Cancer Res. 8 (2) (2018) 317–331.

[7] Why You Should Not Use Ivermectin to Treat or Prevent COVID-19. https://www.fda.gov/consumers/consumer-updates/why-you-should-not-use-ivermectin-treat-or-prevent-covid-19. Accessed data: 02 May 2022.

[8] U.K. Udensi, A.F. Fagbenro-Beyioku, Effect of ivermectin on trypanosoma brucei brucei in experimentally infected mice, J. Vector Borne Dis. 49 (3) (2012) 143–150.

[9] A. Crump, Ivermectin: enigmatic multifaceted 'wonder' drug continues to surprise and exceed expectations, J. Antibiot. (Tokyo) 70 (5) (2017) 495–505, https://doi.org/10.1038/ja.2017.11.

[10] B.D. Foy, H. Alout, J.A. Seaman, S. Rao, T. Magalhaes, M. Wade, S. Parikh, D. D. Soma, A.B. Sagna, F. Fournet, H.C. Slater, R. Bougma, F. Drabo, A. Diabaté, A.G. V. Coulidiaty, N. Rouamba, R.K. Dabiré, Efficacy and risk of harms of repeat ivermectin mass drug administrations for control of malaria (RIMDAMAL): a cluster-randomised trial, Lancet 393 (10180) (2019) 1517–1526, https://doi.org/10.1016/S0140-6736(18)32321-3.

[11] N.S. Kane, B. Hirschberg, S. Qian, D. Hunt, B. Thomas, R. Brochu, S.W. Ludmerer, Y. Zheng, M. Smith, J.P. Arena, C.J. Cohen, D. Schmatz, J. Warmke, D.F. Cully, Drug-resistant Drosophila indicate glutamate-gated chloride channels are targets for the antiparasitics nodulisporic acid and ivermectin, Proc. Natl. Acad. Sci. U. S. A. 97 (25) (2000) 13949–13954, https://doi.org/10.1073/pnas.240464697.

[12] A. Priel, S.D. Silberberg, Mechanism of ivermectin facilitation of human P2X4 receptor channels, J. Gen. Physiol. 123 (3) (2004) 281–293, https://doi.org/10.1085/jgp.200308986.

[13] M. Tang, X. Hu, Y. Wang, X. Yao, W. Zhang, C. Yu, F. Cheng, J. Li, Q. Fang, Ivermectin, a potential anticancer drug derived from an antiparasitic drug, Pharmacol. Res. 163 (2021), 105207, https://doi.org/10.1016/j.phrs.2020.105207.

[14] J. Wang, Y. Xu, H. Wan, J. Hu, Antibiotic ivermectin selectively induces apoptosis in chronic myeloid leukemia through inducing mitochondrial dysfunction and oxidative stress, Biochem. Biophys. Res. Commun. 497 (1) (2018) 241–247, https://doi.org/10.1016/j.bbrc.2018.02.063.

[15] J. Liu, K. Zhang, L. Cheng, H. Zhu, T. Xu, Progress in understanding the molecular mechanisms underlying the antitumour effects of ivermectin, Drug Des. Devel. Ther. 14 (2020) 285–296, https://doi.org/10.2147/DDDT.S237393.

[16] D. Trachootham, J. Alexandre, P. Huang, Targeting cancer cells by ROS-mediated mechanisms: a radical therapeutic approach? Nat. Rev. Drug Discov. 8 (2009) 579–591.

[17] S.C. Gupta, D. Hevia, S. Patchva, B. Park, W. Koh, B.B. Aggarwal, Upsides and downsides of reactive oxygen species for cancer: the roles of reactive oxygen species in tumorigenesis, prevention, and therapy, Antioxid. Redox Signal. 16 (11) (2012) 1295–1322, https://doi.org/10.1089/ars.2011.4414.

[18] M. Fouladvand, A. Barazesh, R. Tahmasebi, Evaluation of in vitro antileishmanial activity of curcumin and its derivatives "gallium curcumin, indium curcumin and diacethyle curcumin", Eur. Rev. Med. Pharmacol. Sci. 17 (24) (2013) 3306–3308.

[19] R. Das, A. Roy, N. Dutta, H.K. Majumder, Reactive oxygen species and imbalance of calcium homeostasis contributes to curcumin induced programmed cell death in Leishmania donovani, Apoptosis 13 (7) (2008) 867–882, https://doi.org/10.1007/s10495-008-0224-7.

[20] M. Elamin, E. Al-Olayan, R. Abdel-Gaber, R.S. Yehia, Anti-proliferative and apoptosis induction activities of curcumin on Leishmania major, Rev. Argent. Microbiol. 53 (3) (2021) 240–247, https://doi.org/10.1016/j.ram.2020.08.004.

[21] B. Tiwari, R. Pahuja, P. Kumar, S.K. Rath, K.C. Gupta, N. Goyal, Nanotized curcumin and miltefosine, a potential combination for treatment of experimental visceral Leishmaniasis, Antimicrob. Agents Chemother. 61 (3) (2017), e01169-16, https://doi.org/10.1128/AAC.01169-16.

[22] P. Liczbiński, J. Michałowicz, B. Bukowska, Molecular mechanism of curcumin action in signaling pathways: review of the latest research, Phytother. Res. 34 (8) (2020) 1992–2005, https://doi.org/10.1002/ptr.6663.

[23] R.A. Moreira, S.A. Mendanha, K.S. Fernandes, G.G. Matos, L. Alonso, M.L. Dorta, A. Alonso, Miltefosine increases lipid and protein dynamics in Leishmania amazonensis membranes at concentrations similar to those needed for cytotoxicity activity, Antimicrob. Agents Chemother. 58 (2014) 3021–3028, https://doi.org/10.1128/AAC.01332-13.

[24] K.S. Fernandes, P.E. de Souza, M.L. Dorta, A. Alonso, The cytotoxic activity of miltefosine against Leishmania and macrophages is associated with dynamic changes in plasma membrane proteins, Biochim. Biophys. Acta 1859 (1) (2017) 1–9, https://doi.org/10.1016/j.bbamem.2016.10.008.

[25] L. Alonso, É.J.S. Cardoso, R.S. Gomes, S.A. Mendanha, M.L. Dorta, A. Alonso, Antileishmanial and cytotoxic activities of ionic surfactants compared to those of miltefosine, Colloids Surf. B Biointerfaces 183 (2019), 110421, https://doi.org/10.1016/j.colsurfb.2019.110421.

[26] H.S. Camargos, R.A. Moreira, S.A. Mendanha, K.S. Fernandes, M.L. Dorta, A. Alonso, Terpenes increase the lipid dynamics in the Leishmania plasma membrane at concentrations similar to their IC50 values, PLoS One. 9 (8) (2014), e104429, https://doi.org/10.1371/journal.pone.0104429.

[27] L. Alonso, K.S. Fernandes, S.A. Mendanha, P.J. Gonçalves, R.S. Gomes, M.L. Dorta, A. Alonso, In vitro antileishmanial and cytotoxic activities of nerolidol are associated with changes in plasma membrane dynamics, Biochim. Biophys. Acta 2019 (1861) 1049–1056, https://doi.org/10.1016/j.bbamem.2019.03.006.

[28] L. Alonso, S.A. Mendanha, M.L. Dorta, A. Alonso, Analysis of the interactions of amphotericin B with the Leishmania plasma membrane using EPR spectroscopy, J. Phys. Chem. B 124 (45) (2020) 10157–10165, https://doi.org/10.1021/acs.jpcb.0c07721.

[29] L. Alonso, S.A. Mendanha, R.S. Gomes, M.L. Dorta, A. Alonso, Comparative EPR spectroscopy analysis of amphotericin B and miltefosine interactions with Leishmania, erythrocyte and macrophage membranes, Eur. J. Pharm. Sci. 163 (2021), 105859, https://doi.org/10.1016/j.ejps.2021.105859.

[30] L. Alonso, R. Menegatti, R.S. Gomes, M.L. Dorta, R.M. Luzin, L.M. Lião, A. Alonso, Antileishmanial activity of the chalcone derivative LQFM064 associated with reduced fluidity in the parasite membrane as assessed by EPR spectroscopy, Eur. J. Pharm. Sci. 151 (2020), 105407, https://doi.org/10.1016/j.ejps.2020.105407.

[31] L. Alonso, J.C. de Paula, P. Baréa, M.H. Sarragiotto, T.U. Nakamura, A. Alonso, N. S. Fernandes, C.A.C. Lancheros, H. Volpato, D.L. Bidóia, C.V. Nakamura, Membrane dynamics in Leishmania amazonensis and antileishmanial activities of β-carboline derivatives, Biochim. Biophys. Acta Biomembranes 1863 (2021), 183473, https://doi.org/10.1016/j.bbamem.2020.183473.

[32] P. Baréa, J.C. de Paula, L. Alonso, A.R. de Oliveira, W.F. da Costa, A. Alonso, C. V. Nakamura, M.H. Sarragiotto, Synthesis, antileishmanial activity and spin labeling EPR studies of novel β-carboline-oxazoline and β-carboline-dihydrooxazine derivatives, J. Braz. Chem. Soc. (2020), https://doi.org/10.21577/0103-5053.20200003.

[33] L. Alonso, K.E. Pianoski, A. Alonso, F.A. Rosa, Antileishmanial activity of 3,4,5-trisubstituted isoxazoles by interaction with Leishmania amazonensis plasma membrane, J. Mol. Struct. 1249 (2022), 131604, https://doi.org/10.1016/j.molstruc.2021.131604.

[34] V.C. Desoti, D. Lazarin-Bidóia, D.B. Sudatti, R.C. Pereira, A. Alonso, T. Ueda-Nakamura, B.P.Dias Filho, C.V. Nakamura, Sde O. Silva, Trypanocidal action of (-)-elatol involves an oxidative stress triggered by mitochondria dysfunction, Mar. Drugs 10 (8) (2012) 1631–1646, https://doi.org/10.3390/md10081631.

[35] G.O. Fruhwirth, A. Loidl, A. Hermetter, Oxidized phospholipids: from molecular properties to disease, Biochim. Biophys. Acta 1772 (7) (2007) 718–736.

[36] A. Catala, Lipid peroxidation of membrane phospholipids generates hydroxy-alkenals and oxidized phospholipids active in physiological and/or pathological conditions, Chem. Phys. Lipids 157 (1) (2009) 1–11.

[37] O. Jovanović, S. Škulj, E.E. Pohl, M. Vazdar, Covalent modification of phosphatidylethanolamine by 4-hydroxy-2-nonenal increases sodium permeability across phospholipid bilayer membranes, Free Radic. Biol. Med. 143 (2019) 433–440, https://doi.org/10.1016/j.freeradbiomed.2019.08.027.

[38] H. Zhong, H. Yin, Role of lipid peroxidation derived 4-hydroxynonenal (HNE) in cancer: focusing on mitochondria, Redox Biol. 4 (2015) 193–199, https://doi.org/10.1016/j.redox.2014.12.011.

[39] G. Poli, R.J. Schaur, W.G. Siems, G. Leonarduzzi, 4-hydroxynonenal: a membrane lipid oxidation product of medicinal interest, Med. Res. Rev. 28 (2008) 569–631.

[40] E.A. Malingriaux, A. Rupprecht, L. Gille, O. Jovanovic, P. Jezek, M. Jaburek, E. E. Pohl, Fatty acids are key in 4-hydroxy-2-nonenal-mediated activation of uncoupling proteins 1 and 2, PLoS One 8 (10) (2013), e77786.

[41] O. Jovanovic, A.A. Pashkovskaya, A. Annibal, M. Vazdar, N. Burchardt, A. Sansone, L. Gille, M. Fedorova, C. Ferreri, E.E. Pohl, The molecular mechanism behind reactive aldehyde action on transmembrane translocations of proton and potassium ions, Free Radic. Biol. Med. 89 (2015) 1067–1076.

[42] L. Alonso, R. Menegatti, M.L. Dorta, A. Alonso, Plasma membrane rigidity effects of 4-hydroxy-2-nonenal in Leishmania, erythrocyte and macrophage, Toxicol. in Vitro 79 (2021), 105294, https://doi.org/10.1016/j.tiv.2021.105294.

[43] S.A. Mendanha, J.L.V. Anjos, A.H.M. Silva, A. Alonso, Electron paramagnetic resonance study of lipid and protein membrane components of erythrocytes oxidized with hydrogen peroxide, Braz. J. Med. Biol. Res. 45 (6) (2012) 473–481, https://doi.org/10.1590/S0100-879X2012007500050.

[44] L.M. Snyder, N.L. Fortier, J. Trainor, J. Jacobs, L. Leb, B. Lubin, D. Chiu, S. Shohet, N. Mohandas, Effect of hydrogen peroxide exposure on normal human erythrocyte deformability, morphology, surface characteristics, and spectrin-hemoglobin cross-linking, J. Clin. Invest. 76 (1985) 1971–1977, https://doi.org/10.1172/JCI112196.

[45] A. Alonso, C.S. Queiroz, A.C. Magalhaes, Chilling stress leads to increased cell membrane rigidity in roots of coffee (Coffea arabica L.) seedlings, Biochim. Biophys. Acta 1323 (1997) 75–84, https://doi.org/10.1016/S0005-2736(96)00177-0.

[46] M.F. Nepomuceno, A. Alonso, L. Pereira-da-Silva, M. Tabak, Inhibitory effect of dipyridamole and its derivatives on lipid peroxidation in mitochondria, Free Radic.

Biol. Med. 23 (1997) 1046–1054, https://doi.org/10.1016/s0891-5849(97)00135-4.
[47] P. Jithavech, P. Suwattananuruk, C.Muangnoi Hasriadi, W. Thitikornpong, P. Towiwat, O. Vajragupta, P. Rojsitthisak, Physicochemical investigation of a novel curcumin diethyl γ-aminobutyrate, a carbamate ester prodrug of curcumin with enhanced anti-neuroinflammatory activity, PLoS One 17 (3) (2022), e0265689, https://doi.org/10.1371/journal.pone.0265689.
[48] Safety Data Sheet - Ivermectin (3.5%) Formulation. https://www.msd.com/docs/product/safety-data-sheets/ah-sds/Ivermectin%20(3.5_pct)%20Formulation_AH_JP_6N.pdf. Accessed data: 02 May 2022.